

Optical Switching of Protein Interactions on Photosensitive–Electroactive Polymers measured by Atomic Force Microscopy

Amy Gelmi¹, Michele Zanoni², Michael J. Higgins^{1*}, S. Gambhir¹,
D. L. Officer¹, Dermot Diamond^{2*}, Gordon G. Wallace¹

¹*ARC Centre of Excellence for Electromaterials Science, Intelligent Polymer Research Institute, University of Wollongong, Wollongong, NSW 2522, Australia*

²*CLARITY: Centre for Sensor Web Technologies, National Centre for Sensor Research, Dublin City University, Dublin 9, Ireland*

Received Date:

Title Running Head: Optical Switching of Protein Adhesion

**Corresponding authors.*

Dr Michael Higgins

Email: mhiggins@uow.edu.au

Tel: +61-2-4221-3989

Fax: +61-2-4221-3114

Prof. Dermot Diamond

Email: dermot.diamond@dcu.ie

Abstract

The ability to switch the physico-chemical properties of conducting polymers opens up new possibilities for a range of new applications. Appropriately functionalised materials can provide routes to multi-modal switching, for example in response light and/or electrochemical stimuli; this capability is important in the field of bionics, wherein remote control of the properties of materials opens new possibilities. For example, the ability to actuate a film via photonic stimuli is particularly interesting as it facilitates the modulation of interactions between surface host binding sites and potential guest molecules. In this work, we studied two different poly-terthiophenes: one was functionalized with a spiropyran photoswitch (pTTh-SP) and the second with a non-photoswitchable methyl acetate moiety (pTTh-MA). These substrates were exposed to several cycles of illumination with light of different wavelengths and the resulting effect studied with UV-*vis* spectroscopy, contact angle and atomic force microscopy (AFM). The AFM tips were chemically activated with fibronectin (FN) and the adhesion force of the protein to the polymeric surface was measured. The pTTh-MA (no SP incorporated) showed a slightly higher average maximum adhesion (0.96 ± 0.14 nN) than the modified pTTh-SP surface (0.77 ± 0.08 nN), but after exposure of the pTTh-SP polymer to UV, the average maximum adhesion of the pTTh-MC was significantly smaller (0.49 ± 0.06 nN) than both the pTTh-MA and pTTh-SP. These results suggest that hydrophobic forces are predominant in determining the protein adhesion to the films studied and that this effect can be photonically tuned. By extension, this further implies that it should be possible to obtain a degree of spatial and temporal control of the surface binding behaviour of certain proteins with these functionalised surfaces through photo-activation/deactivation, which, in principle, should facilitate patterned growth behaviour (e.g. using masks or directional illumination) or photocontrol of protein uptake and release.

Keywords: Spiropyran, Conducting Polymer, Polyterthiophene, Atomic Force Microscopy, Protein Adhesion, Fibronectin

Introduction

Switchable surfaces offer control over the material interface via an external stimulus, including light, temperature, pH and electrical field, which can be applied either as a ‘one-off’ or a reversible change [1]. For cell-based applications, switchable materials offer the ability to control interactions at the cell-material interface. In particular, the switching of protein adsorption and conformation can be used to modulate cellular proliferation and differentiation [1-3]. Light switching in ‘once-off’ switching materials can promote specific biomolecular adhesion to the surface [4], while electrical switching is particularly applicable to organic conductors (e.g. CNT, conducting polymers) and shown to enhance cell growth and differentiation [5-10]. In biosensing applications, however, the surface adsorption of proteins is undesirable and decreases the efficacy of the device [11-13]. A dynamic material that controls both the adsorption and desorption of proteins and living cells opens up several possibilities in patterned cell growth, tissue engineering, and biosensing applications [14-16].

Polymer-based materials have been designed to take advantage of switchable properties for the above applications [17-20]. Polymers can be switched through a variety of external stimuli that typically provide a single pathway to control the interfacial response. A developing area in the field of switchable materials is the implementation of multiple stimuli via copolymers as this provides increased flexibility in the manner by which the interfacial behaviour is controlled. This in turn is important for applications wherein both spatial and temporal control over surface interactions is desired. For example, a material comprising both thermoresponsive poly(N-isopropylacrylamide) (pNIPAM) and photoresponsive

spirobenzopyran (SP) enables both control over the spatial direction of cellular growth with UV light and the removal of cells via low temperature washing [14]. This strategy has been taken a step further by combining light, temperature, and pH to control tuneable microgels comprising a temperature/pH sensitive pNIPAM-allylamine copolymer microgel functionalized with the SP photosensitive molecule [21]. In this case, the optical properties of the copolymer changed the thermal threshold for volume changes of the microgel, as well as a photochromic change when switched. The amine groups in the microgel were pH sensitive and reduced swelling capability with an increase in pH.

When designing a material with bi-modal switching capabilities, the incorporation of photoswitchability is often attractive as it enables fast, non-invasive, and highly controllable switching with spatial resolution. Photocleavable groups that are actively switched via specific wavelengths of light have previously been used to inhibit or facilitate cell adhesion [4]. This type of switching induces an irreversible change but despite this, it is useful for surface patterning or release of molecules (e.g. drug delivery) [22]. The second common optical switching mechanism is photoisomerisation wherein the molecule undergoes heterolytic bond cleavage producing an isomer that will have a different polarity to the original molecule. SP is commonly used in this regard as it undergoes a heterolytic cleavage of the spiro carbon-oxygen bond to create an open ringed structure that has two resonance merocyanine-like and quinoidal-like MC forms. SP has been studied in combination with temperature responsive pNIPAM polymers to produce photosensitive copolymer materials [22-24]. They have also been incorporated as a copolymer with methyl methacrylate to produce a photosensitive poly(spiropyran-*co*-methyl methacrylate) material that upon switching from the SP to MC form can induce the detachment of platelets and mesenchymal stem cells [25]. The SP molecule has also been incorporated into materials such as self-

assembled monolayers [26], bilayers [27], polymers [28], and more recently organic conducting polymers [29-30].

A novel organic conducting polymer, a polyterthiophene with SP attached to the polymer backbone, has recently been synthesized to produce a photosensitive conductive polymer [29a]. The SP was covalently bound to the alkoxyterthiophene monomer units to produce the polymer poly(2-(3,3"-dimethylindoline-6'-nitrobenzospiropyranyl)ethyl 4,4"-didecyloxy-2,2':5',2"-terthiophene-3-acetate). Electrical switching of the polythiophene backbone showed good reversibility and stability and additional photoswitching of the SP moiety was possible using optical stimulus. Figure 1A shows the chemical structure of the polymer and reversible transition between the SP and MC forms as a function of UV/visible light switching. While the effect of both light and electrical switching on the redox properties and SP-to-MC conversion was investigated, the material was not exploited to demonstrate control over the physical interactions of proteins or living cells.

In this study, we focused on the effect of optical stimulation on the poly(2-(3,3"-dimethylindoline-6'-nitrobenzospiropyranyl)ethyl 4,4"-didecyloxy-2,2':5',2"-terthiophene-3-acetate) (termed pTTh-SP) polymer described in our above study [29a] to investigate the ability to control fibronectin (FN) protein adhesion, which is an important interaction within extracellular matrix for mediating cell adhesion. In order to support cell adhesion and signalling via $\alpha_5\beta_1$ integrin binding receptors to RGD sites within FN, the protein must be in the appropriate conformation whilst possessing adhesion to the substrate. FN binding to cell integrin receptors triggers the formation of actin stress fibres that promotes cell adhesion and proliferation. Subsequent cell signalling is modulated through a continuum of mechanical

forces (i.e. mechanotransduction) and thus is dependent on the strength of FN adhesion to a surface.

Materials and Methods

The molecules used for this study (pTTh-MA and pTTh-SP) were synthesized and then electro-polymerised according to the procedure previously reported [29a]. The electrodes selected were the optically transparent ITO (Indium Tin Oxide) coated glass (Delta Technologies, Limited, resistivity $R_s=4-8 \Omega$). Absorbance spectra were recorded using a Shimadzu UV-1800 spectrophotometer. The polymers were washed in acetonitrile after the polymerisation in order to remove the excess of electrolyte and the absorbance spectra measured. The absorbance spectra was then measured for the pTTh-SP exposed to UV (254 nm) light for 5 min, and then once exposed to visible light (full spectrum) for 5 min. The pTTh-SP was then exposed to UV light for 15 min and the absorbance spectra measured. All light switching was performed at room temperature.

Four different freshly polymerised films (stored at -0.4 V) were subjected to 5 cycles of exposure to UV light (254 nm, 15 min) and 5 cycles of exposure to visible light (full spectrum, 15 min). After each exposure, contact angles were obtained for each film in triplicate.

The functionalization precursors 3-ethoxydimethylsilylamine propyl (3-EDSPA) and glutaraldehyde (GAH) were obtained from Sigma Aldrich. Human plasma fibronectin (FN) was obtained from Sigma Aldrich. Phosphate buffer saline (PBS) was prepared at pH 7 in Milli-Q water (18.2M Ω). The tip is functionalized using an aminosilanization method to covalently bind the protein to the tip. Silicon nitride tips are used for this method due to the

availability of silicon oxide groups on the surface. The tips were initially prepared with a plasma cleaner to remove any impurities or functionalized groups on the surface. Once cleaned the tips were immediately functionalized to minimise contaminants on the surface. The tips were placed into the 3-EDSPA solution at room temperature for 1 h. The tips were then removed, washed consecutively with toluene and then in PBS solution. The tips were then immersed in the GAH solution for 1 h and then rinsed with PBS solution. The tips were finally immersed in the FN solution for 1 h, then rinsed and refrigerated in PBS solution until use. The AFM parameters for the force measurements were set to 500 nm for the z-distance, 0.5 Hz scan rate, 1 s dwell toward the surface, and 1 nN trigger force. Single point force spectroscopy measurements were performed with 5 consecutive measurements at one point, with a rest of 3 s, across 5 different points on the sample surface. 25 force curves were performed by 3 individual tips on 3 samples for measurements on pTTh-MA and pTTh-SP (total number of force curves 228 and 200 on pTTh-MA and pTTh-SP, respectively).

The modified polymers were switched using optical stimulation to measure protein adhesion on the SP and MC form. The polymer was irradiated with UV light (wavelength 254 nm) for 10 min in order to switch it from pTTh-SP to pTTh-MC in PBS solution. The polymer was then exposed to room light for 10 min to switch from pTTh-MC to pTTh-SP. Force spectroscopy measurements were performed with 5 consecutive measurements at one point, with a rest of 3 s, across 5 different points on the sample surface. 25 force curves were performed on the polymer after the light stimulation was applied and 4 samples with 4 individual tips were used (total number of force curves 200 and 150 for SP and MC form respectively).

Contact angle experiments on the polymer surfaces were obtained with a First Ten Ångströms FTA200 analyser at room temperature and environment humidity, using water as the probe liquid. The pTTh-SP polymer was initially electrically stimulated at a constant -0.4 V after polymerisation in 0.1 M TBAP electrolyte (acetonitrile solvent) in order to guarantee the higher concentration possible of the SP isomer, subjected to the illumination cycles as previously described and then analysed with the contact angle. Six freshly synthesised samples of pTTh-MA were washed in acetonitrile to remove the excess of electrolyte. Three of them were electrically stimulated at -0.4V and the other three were kept at 0.9V and then tested with the contact angle analyser.

Results and Discussion

UV-Vis Spectra

The UV-vis absorbance spectra for the switching pTTh-SP is shown in Figure 1B. The fully switched, oxidised pTTh-SP polymer was initially measured (blue). The polymer was then switched to the MC form by exposure to UV light (red) and then switched back to the SP form again (green). The polymer was switched to MC a final time (purple). The absorbance spectra shows a shift with the optical stimulation, indicating that the polymer is undergoing photoisomerisation.

Contact Angle Measurements

The optical stimulation was shown to induce a change in the wettability of the pTTh-SP functionalized polymer, as demonstrated by the contact angle measurements. As a control,

optical stimulation did not produce any effect on the SP-free pTTh-MA polymer. Figure 1C displays the average contact angle measurement as the polymer is optically switched from SP to MC form five times. The measurements show a stable, reversible change of the contact angle of the polymer. The SP form is the more hydrophobic form (an average contact angle of $100.0 \pm 5.6^\circ$), and the MC form is more hydrophilic (an average contact angle of $84.3 \pm 2.5^\circ$). The hydrophobic nature of SP has previously been related to its chemical structure [24, 31] and similarly confirmed using contact angle measurements [25]. The weaker hydrophobicity of the MC form is attributed to its zwitterionic structure that forms due to cleavage of the spiro carbon-oxygen bond and results in the heterolysis of the nitrogen and oxygen (Figure 1A) [31]. Furthermore, the contact angle measurements demonstrated that the change in wettability was reversible upon cycling of the optical switching and agrees with a previous study on the reversible optical switching properties of the SP [32].

Protein Adhesion

The interaction of FN with the polymer was measured using AFM force spectroscopy, as depicted in Figure 2A. In these measurements, a chemically functionalized FN tip is brought into contact, and then withdrawn from, the polymer surface whilst measuring the tip-sample adhesive forces as a function of optical stimulation. A typical force curve on the pTTh-MA polymer with no SP incorporated and without optical stimulation shows a large peak upon retraction of the tip, indicating the presence of an adhesive interaction between the FN and polymer (Figure 2B). The strength of protein adhesion is given as the peak maximum (Figure 2B, vertical arrow), which is on the order of nanonewtons (~ 1 nN). This type of adhesion is typically due to the interaction of several proteins on the tip, involving both intra and inter-protein interactions, and their subsequent detachment from the surface. Inter-protein

interactions may include electrostatic, hydrophobic and hydrogen bonding, while inter-protein interactions include unfolding of the protein or adhesion between proteins, all of which may contribute to the strength or energy (integral of area under peak) of protein adhesion. The pTTh-MA showed a slightly higher average maximum adhesion (0.96 ± 0.14 nN) than the modified pTTh-SP surface (0.77 ± 0.08 nN), as displayed in Figure 2C. After exposure of the pTTh-SP polymer to UV, the average maximum adhesion of the pTTh-MC was significantly smaller (0.49 ± 0.06 nN) than both the pTTh-MA and pTTh-SP. When comparing the change in surface energy (contact angle) and adhesion, both parameters show a decrease in the order of pTTh-MA > SP > MC, suggesting that an increase in hydrophilicity (or conversely a decrease in hydrophobicity) correlates with a decrease in protein adhesion. Based on this correlation, it appears that hydrophobic interactions may be the dominant forces involved in protein adhesion. The increased hydrophobicity of the pTTh-MA is due to its neutral backbone, in addition to the presence of polar decyloxy and acetate groups. This is in contrast to the pTTh-SP where the nitro groups will contribute to hydrophilicity. The reduction in hydrophobicity of the MC form is attributed to the zwitterionic nature of the MC molecule, which has previously been shown to also reduce protein adhesion [33-34]. Zwitterionic surfaces are believed to be resistant to non-specific protein adhesion due to hydration layer(s) bound through solvation of charged terminal groups, as well as hydrogen bonding around molecular chains [35]. This switch to the more hydrophilic MC form with zwitterionic species may either diminish the extent of hydrophobic interactions and/or play a role in actually deterring protein adhesion.

Figure 3A displays the reversibility in protein adhesion as the polymer is switched between the SP and MC forms. Representative force curves on pTTh-SP demonstrate a much higher adhesion force (larger peaks) compared to pTTh-MC, clearly indicating a reversible effect of

the optical stimulus on protein adhesion. Figure 3B shows the average maximum adhesion force of the SP and MC forms as they are reversibly switched over 2 cycles. The initial SP form (electrically stimulated to ensure complete conversion to the SP form) was measured to have a mean of 0.91 ± 0.04 nN (mean \pm s.d., $n=50$). The first switch to pTTh-MC with UV light reduced the mean maximum adhesion to 0.31 ± 0.01 nN (mean \pm s.d., $n=75$). The first switch back to pTTh-SP with visible light measured an increase in the mean maximum adhesion to 0.67 ± 0.03 (mean \pm s.d., $n=150$) and the second switch to pTTh-MC with UV light decreased the mean again to 0.46 ± 0.01 (mean \pm s.d., $n=75$). The reversibility of the protein adhesion exhibits a small amount of hysteresis as the switching is performed over multiple cycles. In particular, the average adhesion force of the SP does not return to its initial value (27% reduction in the average adhesion force) after switching back from the MC form, suggesting that not all of the MC isomers undergo switching back to the SP form. As the force measurements are not performed simultaneously during the optical switching (i.e. only before or after switching is performed), the measurements may be susceptible to time-dependent (e.g. 'lag' time) changes in the SP-to-MC conversion.

A previous study using a copolymer of nitrobenzospiropyran and methyl methacrylate has shown that the amount of adsorbed fibrinogen protein on SP surfaces and those surfaces already in the MC form is almost comparable, even though the MC form results in a significant decrease in contact angle (increased hydrophilicity) [25]. In the same study, however, it was shown that the amount of adsorbed fibrinogen on SP surfaces significantly decreases when those same surfaces are exposed to UV irradiation, suggesting that the physical movement associated with the molecular switching, rather than a change in surface energy, is primarily responsible for inducing protein detachment. This detachment of the fibrinogen was also related to the ability to induce detachment of platelet cells [25]. The AFM

force spectroscopy measurements in our study are analogous to the situation where the direct measurement of protein adhesion is made on surfaces already in the SP and MC form, thus limiting any effects to only the static properties of the surfaces. Therefore, contrary to the above study, we observe a significant difference in protein adhesion between the PTTh-MA, SP and MC forms that correlates with a change in their surface energy. Specifically, the protein adhesion decreases with an increase in hydrophilicity. Conversely, UV irradiation of a spiropyran–poly(N-isopropylacrylamide) copolymer prior to low temperature washing was shown to promote the adhesion of CHO-K1 cells, suggesting an attractive interaction between the zwitterionic isomer and cell membrane that also has zwitterionic groups, although the surface energies, switching mechanisms of the copolymer, or influence on protein adhesion were not addressed in the study [14]. The findings from the above different studies highlight the potential complexities and differences in underlying mechanisms for controlling protein and cell interactions using optical stimulation, particularly in dual stimuli systems where the photosensitive SP is combined with another polymer constituent that may be electroactive, temperature sensitive or simply of different surface chemistry.

During the adhesive interaction of the FN, the maximum extension length, or elongation, of the protein(s) is given as the distance on the x-axis (i.e. tip-sample separation distance) where the protein eventually detaches from the surface and the force returns to zero (Figure 2B, horizontal arrow). Histograms showing the distribution of the protein extension lengths did not show any significant difference between the SP and MC forms of the polymer (Figure 4). Mean peak distribution values for the pTTh-SP (Figure 4A) and pTTh-MC (Figure 4B) were 24.9 ± 0.8 nm and 21.9 ± 2.3 nm, respectively. These extension lengths, which are significantly smaller than the theoretical and experimentally observed 160-180 nm contour length of FN in its extended conformation [36-39], indicate that the protein interaction is

occurring over a distance more closely related to the average dimensions of FN in its compact conformation (i.e. $\approx 20 \text{ nm} \times 15 \text{ nm}$) [36]. These extension lengths of $\approx 25 \text{ nm}$ for the pTTh-SP and pTTh-MC are also much shorter than the distribution of extension lengths, 60 nm, 120 nm and 160-175 nm, observed in our recent AFM study on FN interactions with the conducting polymer, polypyrrole, doped with glycosaminoglycans (GAGs) such as chondroitin sulfate, hyaluronic acid and dextran sulfate [40]. In this case, the presence of the GAGs, which are large, highly negatively charged polyelectrolytes, dramatically increases the surface hydrophilicity (contact angles of $<22^\circ$) [41] and causes the FN to adopt a more extended conformation during its interaction with the polymer [40]. It well-known that the wettability of a surface is important for controlling the conformation of FN. On hydrophobic surfaces, FN adopts a compact, 'pretzel' conformation that is stabilized by intermolecular bonds but can be disrupted by interacting surface groups of hydrophilic and negatively charged surfaces, causing the protein to adopt an extended conformation [42]. Hence, for the hydrophobic pTTh-SP and pTTh-SP polymers ($\text{CA} = 85\text{-}100^\circ$), the observed extension lengths suggest that the FN protein retains its compact conformation during adhesive interactions with the surface.

Conclusion

The switchable nature of the copolymer in this study and its effect on protein adhesion as well as conformation suggest a potential use in priority-driven cellular adhesion to control cell growth, spatially and directionally. This has been demonstrated previously for controlling cell detachment [14] but the ability to resolve reversible, protein interactions with resolution comparable to the nanoscale, as done in this study and others [40], provides significant

insight into the possibilities of exerting fine, molecular level control over cellular interactions.

Acknowledgements: This work has been supported by the Australian Research Council under the Australian Research Fellowship and DP110104359 (Dr Michael Higgins) and ARC Federation Fellowship of Prof. Gordon Wallace. We also greatly acknowledge the Australian National Fabrication Facility (ANFF) for providing Atomic Force Microscopy instrumentation.

MZ and DD acknowledge funding from Science Foundation Ireland (SFI) under the CLARITY CSET award (Grant 07/CE/I1147). We also acknowledge support from the European Commission for funding under grant PIRSES- GA-2010-269302.

References:

1. Cole, M.A., N.H. Voelcker, H. Thissen, and H.J. Griesser, *Stimuli-responsive interfaces and systems for the control of protein–surface and cell–surface interactions*. *Biomaterials*, 2009. **30**(9): p. 1827-1850.
2. García, a.J., M.D. Vega, and D. Boettiger, *Modulation of cell proliferation and differentiation through substrate-dependent changes in fibronectin conformation*. *Molecular Biology of the Cell*, 1999. **10**(3): p. 785-98.

3. Keselowsky, B.G., D.M. Collard, and A.J. García, *Surface chemistry modulates fibronectin conformation and directs integrin binding and specificity to control cell adhesion*. Journal of Biomedical Materials Research, 2003. **66A**(2): p. 247-59.
4. Nakanishi, J., et al., *Photoactivation of a substrate for cell adhesion under standard fluorescence microscopes*. Journal of the American Chemical Society, 2004. **126**(50): p. 16314-16315.
5. Thompson, B.C., et al., *Conducting polymers, dual neurotrophins and pulsed electrical stimulation — Dramatic effects on neurite outgrowth*. Journal of Controlled Release, 2010. **141**(2): p. 161-167.
6. Wong, J.Y., R. Langert, and D.E. Ingber, *Electrically conducting polymers can noninvasively control the shape and growth of mammalian cells*. Science, 1994. **91**(8): p. 3201-3204.
7. Kotwal, A. and C.E. Schmidt, *Electrical stimulation alters protein adsorption and nerve cell interactions with electrically conducting biomaterials*. Biomaterials, 2001. **22**(10): p. 1055-1064.
8. Liu, X., K.J. Gilmore, S.E. Moulton, and G.G. Wallace, *Electrical stimulation promotes nerve cell differentiation on polypyrrole/poly (2-methoxy-5 aniline sulfonic acid) composites*. Journal of Neural Engineering, 2009. **6**(6): p. 065002.
9. Rowlands, A.S. and J.J. Cooper-White, *Directing phenotype of vascular smooth muscle cells using electrically stimulated conducting polymer*. Biomaterials, 2008. **29**(34): p. 4510-4520.
10. Schmidt, C.E., V.R. Shastri, J.P. Vacanti, and R. Langer, *Stimulation of neurite outgrowth using an electrically conducting polymer*. Proceeding of the National Academy of Sciences, 1997. **94**(17): p. 8948-8953.
11. Morra, M. and C. Cassineli, *Non-fouling properties of polysaccharide-coated surfaces*. Journal of Biomaterials Science, Polymer Edition, 1999. **10**(10): p. 1107-1124.
12. Haimovich, B., et al., *A new method for membrane construction on ePTFE vascular grafts: Effect on surface morphology and platelet adhesion*. Journal of Applied Polymer Science, 1997. **63**(11): p. 1393-1400.
13. Sung, W.J. and Y.H. Bae, *A glucose oxidase electrode based on polypyrrole with polyanion/PEG/enzyme conjugate dopant*. Biosensors and Bioelectronics, 2003. **18**(10): p. 1231-1239.
14. Edahiro, J.-i., et al., *In situ control of cell adhesion using photoresponsive culture surface*. Biomacromolecules, 2005. **6**(2): p. 970-974.

15. Jagur-Grodzinski, J., *Polymers for tissue engineering, medical devices, and regenerative medicine. Concise general review of recent studies*. Polymers for Advanced Technologies, 2006. **17**(6): p. 395-418.
16. Yasuda, A., et al., *In vitro culture of chondrocytes in a novel thermoreversible gelation polymer scaffold containing growth factors*. Tissue Engineering, 2006. **12**(5): p. 1237-1245.
17. Auernheimer, J., C. Dahmen, U. Hersel, A. Bausch, and H. Kessler, *Photoswitched cell adhesion on surfaces with RGD peptides*. Journal of the American Chemical Society, 2005. **127**(46): p. 16107-16110.
18. Kwon, O.H., A. Kikuchi, M. Yamato, Y. Sakurai, and T. Okano, *Rapid cell sheet detachment from Poly(N-isopropylacrylamide)-grafted porous cell culture membranes*. Journal of Biomedical Materials Research, 2000. **50**(1): p. 82-89.
19. Hyeong Kwon, O., A. Kikuchi, M. Yamato, and T. Okano, *Accelerated cell sheet recovery by co-grafting of PEG with PIPAAm onto porous cell culture membranes*. Biomaterials, 2003. **24**(7): p. 1223-1232.
20. Uhlmann, P., et al., *In-Situ Investigation of the Adsorption of Globular Model Proteins on Stimuli-Responsive Binary Polyelectrolyte Brushes†*. Langmuir, 2006. **23**(1): p. 57-64.
21. Garcia, A., et al., *Photo-, thermally, and pH-responsive microgels*. Langmuir, 2006. **23**(1): p. 224-229.
22. Shimoboji, T., et al., *Photoresponsive polymer-enzyme switches*. 2002, National Academy of Sciences. p. 16592-16596.
23. Ivanov, A.E., N.L. Eremeev, P.O. Wahlund, I.Y. Galaev, and B. Mattiasson, *Photosensitive copolymer of N-isopropylacrylamide and methacryloyl derivative of spiropyrans*. Polymer, 2002. **43**(13): p. 3819-3823.
24. Sumaru, K., M. Kameda, T. Kanamori, and T. Shinbo, *Characteristic phase transition of aqueous solution of poly(N-isopropylacrylamide) functionalized with spiropyrans*. Macromolecules, 2004. **37**(13): p. 4949-4955.
25. Higuchi, A., et al., *Photon-modulated changes of cell attachments on poly(spiropyran-co-methyl methacrylate) membranes*. Biomacromolecules, 2004. **5**(5): p. 1770-1774.
26. Katsonis, N., M. Lubomska, M.M. Pollard, B.L. Feringa, and P. Rudolf, *Synthetic light-activated molecular switches and motors on surfaces*. Progress in Surface Science, 2007. **82**(7-8): p. 407-434.

27. Seki, T. and K. Ichimura, *Thermal-isomerization behaviors of a spiropyran in bilayers immobilized with a linear polymer and a smectitic clay*. *Macromolecules*, 1990. **23**(1): p. 31-35.
28. Stitzel, S., R. Byrne, and D. Diamond, *LED switching of spiropyran-doped polymer films*. *Journal of Materials Science*, 2006. **41**(18): p. 5841-5844.
29. (a) Wagner, K., et al., *A multiswitchable poly(terthiophene) bearing a spiropyran functionality: Understanding photo- and electrochemical control*. *Journal of the American Chemical Society*, 2011. **133**(14): p. 5453-5462. (b) M. Zanoni, S. Coleman, K.J. Fraser, R. Byrne, K. Wagner, S. Gambhir, D. L. Officer, G. G. Wallace and D. Diamond, *Physicochemical Study of Spiropyran-terthiophene Derivatives: Photochemistry and Thermodynamics*, *Physical Chemistry Chemical Physics*, **2012**, *14*, 9112- 9120.
30. Bardavid, Y., I. Goykhman, D. Nozaki, G. Cuniberti, and S. Yitzchaik, *Dipole assisted photogated switch in spiropyran grafted polyaniline nanowires*. *Journal of Physical Chemistry C*, 2011. **115**(7): p. 3123-3128.
31. Irie, M., K. Hayashi, and A. Menju, *Photoresponsive polymers IV. Photocontrol of viscosity and pH-value in aqueous systems using poly(methacrylic acid) having spirobenzopyran side groups*. *Polymer Photochemistry*, 1981. **1**(3): p. 233-242.
32. Joseph, G., J. Pichardo, and G. Chen, *Reversible photo-/thermoreponsive structured polymer surfaces modified with a spirobenzopyran-containing copolymer for tunable wettability*. *Analyst*, 2010. **135**(9): p. 2303-2308.
33. Olenych, S.G., M.D. Moussallem, D.S. Salloum, J.B. Schlenoff, and T.C.S. Keller, *Fibronectin and cell attachment to cell and protein resistant polyelectrolyte surfaces*. *Biomacromolecules*, 2005. **6**(6): p. 3252-3258.
34. Chen, S., J. Zheng, L. Li, and S. Jiang, *Strong resistance of phosphorylcholine self-assembled monolayers to protein adsorption: Insights into nonfouling properties of zwitterionic materials*. *Journal of the American Chemical Society*, 2005. **127**(41): p. 14473-14478.
35. Ladd, J., Z. Zhang, S. Chen, J.C. Hower, and S. Jiang, *Zwitterionic polymers exhibiting high resistance tononspecificprotein adsorption from human serum and plasma*. *Biomacromolecules*, 2008. **9**(5): p. 1357-1361.
36. M. L. Smith, D. Gourdon, W. C. Little, K. E., Kubow, R. Andresen Eguiluz, S. Luna-Morris, V. Vogel. *PLOS Biol.* 2007, **5**, p: 2243-2254.
37. Erickson, H.P., N. Carrell, and J. McDonagh, *Fibronectin molecule visualized in electron microscopy: a long, thin, flexible strand*. *Journal of Cell Biology*, 1981. **91**: p. 673-678.

38. Erickson, H.P., *Reversible unfolding of fibronectin type III and immunoglobulin domains provides the structural basis for stretch and elasticity of titin and fibronectin*. 1994. **91**: p. 10114-10118.
39. Mao, Y. & Schwarzbauer, J. E. *Fibronectin fibrillogenesis, a cell-mediated matrix assembly process*. Matrix Biology, 2005, **24**, p. 389-399.
40. Gelmi, A., Higgins, M. J., Wallace, G. G.. *Resolving sub-molecular binding and Electrical switching mechanisms of single proteins at electroactive conducting polymers*, Small, **2012** (accepted)
41. K.J. Gilmore, M. Kita, Y. Han, A. Gelmi, M.J. Higgins, S.E. Moulton, G.M. Clark, R. Kapsa and G.G. Wallace, *Skeletal muscle cell proliferation and differentiation on polypyrrole substrates doped with extracellular matrix components*, Biomaterials, 2009, **30**(29), p. 5292-5304
42. Bergkvist, M., J. Carlsson, and S. Oscarsson, *Surface-dependent conformations of human plasma fibronectin adsorbed to silica, mica, and hydrophobic surfaces, studied with use of Atomic Force Microscopy*. Journal of Biomedical Materials Research, 2003. **64A**(2): p. 349-56.

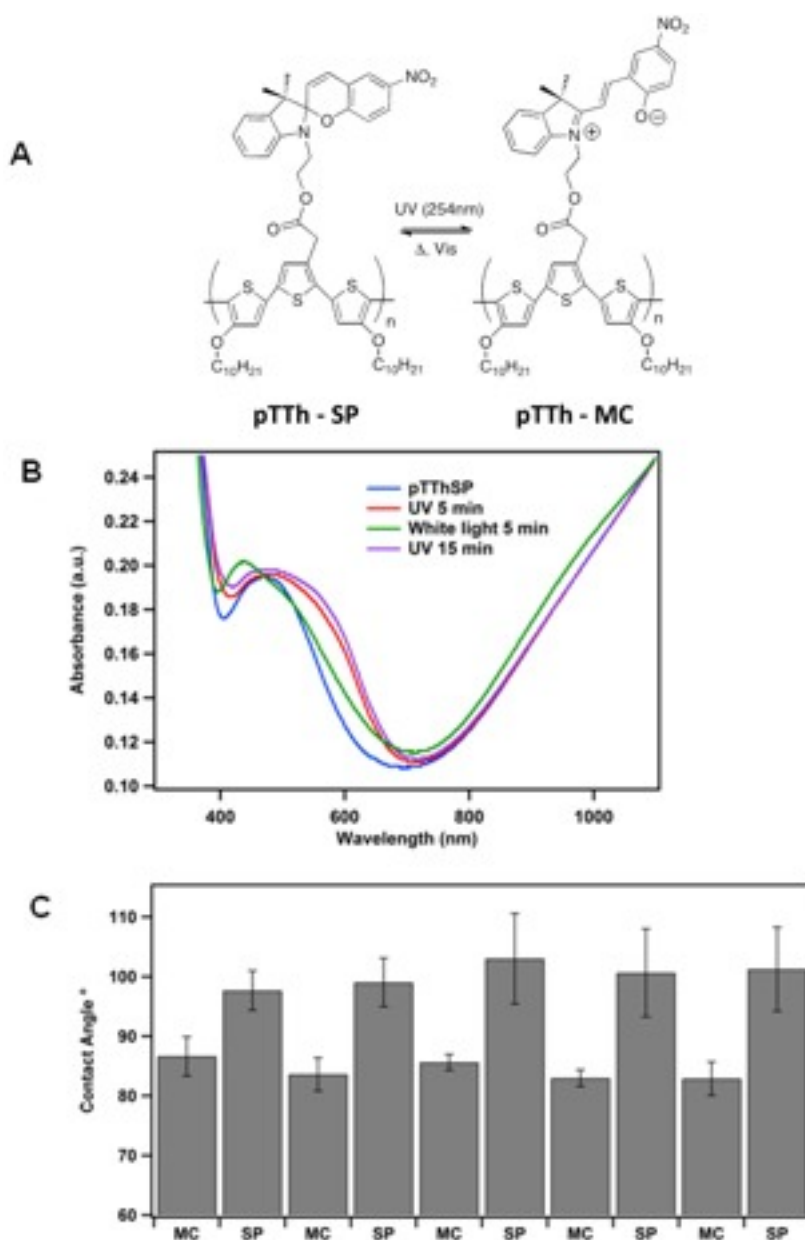


Figure 1: (A) (left structure) Spiropyran covalently bound to alkoxyterthiophene monomer units to produce the polymer poly(2-(3,3"-dimethylindoline-6'-nitrobenzospiropyranyl)ethyl 4,4"-didecyloxy-2,2':5',2"-terthiophene-3-acetate) (termed pTTh-SP) and (right structure) after light switching to the zwitter-ionic isomer in open form (termed pTTh-MC). (B) UV-vis spectra of initial pTTh-SP (blue), UV stimulated 5 min (red), white light stimulated 5 min

(green) and UV stimulated 15 min (purple). (C) Contact angle measurements on polymer as it is optically switched, measured on 4 individual films, cycled 5 times. Error bars are standard deviation.

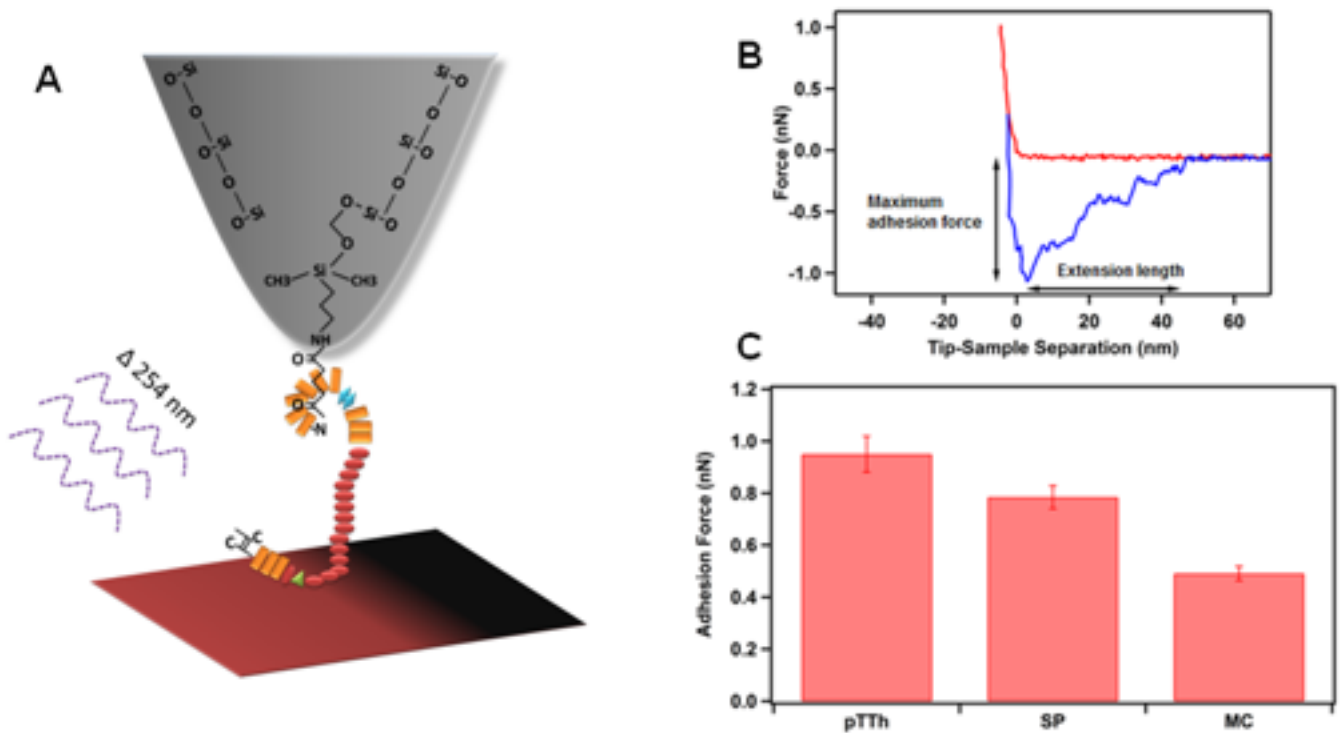
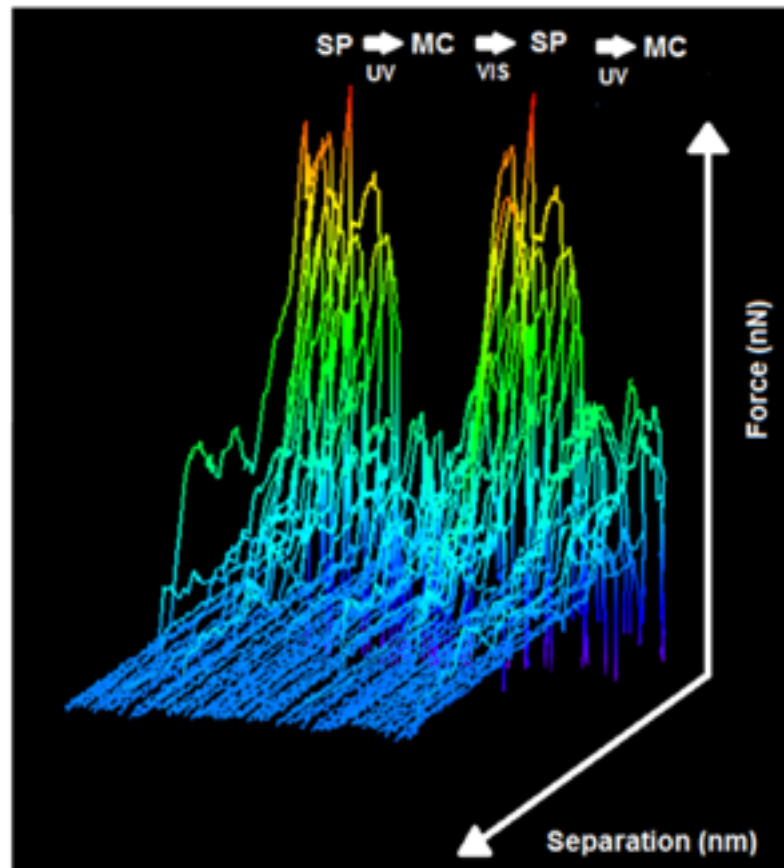


Figure 2: (A) Schematic diagram of AFM tip functionalized with FN interacting with a chromophoric surface stimulated with UV light (wavelength 254 nm). (B) Example force curve analysis, extension (red) and retraction (blue) curves. (C) Average adhesion forces for

as-grown pTTh-MA (n=228), SP (n=200) and MC form (n=150). Error bars are standard error.

A



B

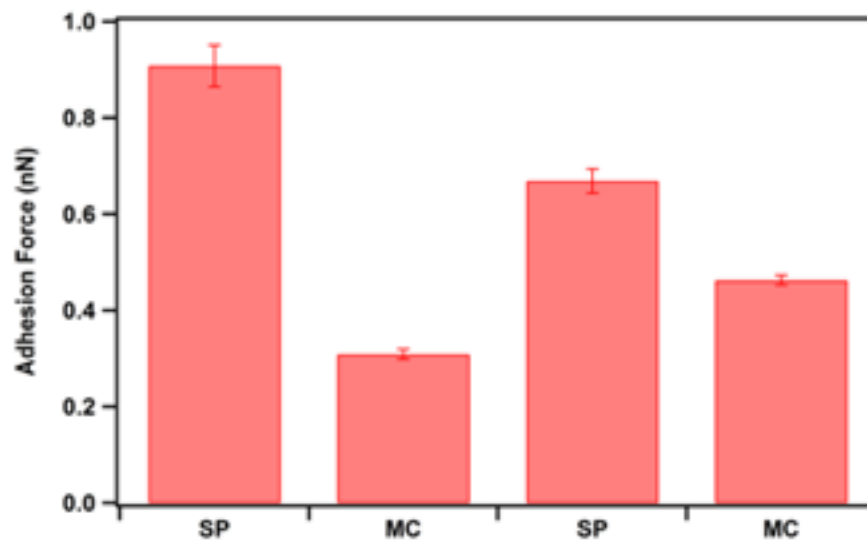


Figure 3: (A) Representative force curves during optical switching. Maximum force 2.4 nN, maximum tip-sample separation 100 nm. (B) Average adhesion forces during optical switching ($n = 50, 75, 150, 75$). Error bars are standard error.

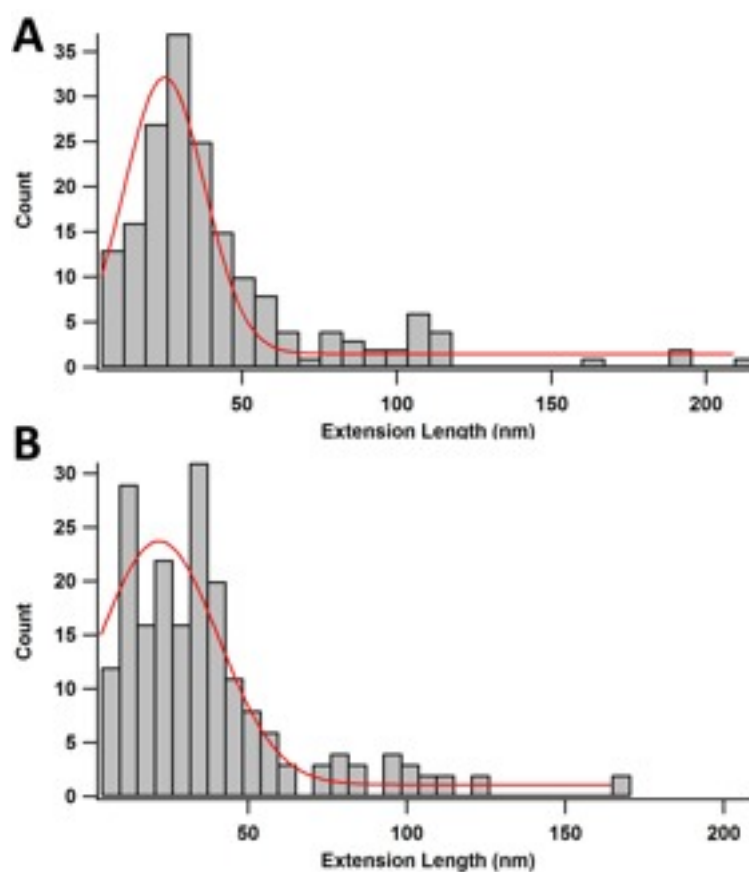


Figure 4. Distribution of extension length for SP (A) and MC (B), $N=180$ and $N=198$ respectively. Red curves are individual gaussian fits.